Inorganic Chemistry

Article

pubs.acs.org/IC

Preparation, Structure, and Properties of Tetranuclear Vanadium(III) and (IV) Complexes Bridged by Diphenyl Phosphate or Phosphate

Kyouhei Sato,[†] Tetsuya Ohnuki,[†] Haruka Takahashi,[†] Yoshitaro Miyashita,[‡] Koichi Nozaki,[†] and Kan Kanamori*,[†]

[†]Department of Chemistry, Graduate School of Science and Engineering, University of Toyama, 3190 Gofuku, Toyama 930-8555, Japan

[‡]Department of Applied Chemistry, Kobe City College of Technology, 8-3 Gakuenhigashimachi, Nishi-ku, Kobe 651-2194, Japan

Supporting Information

ABSTRACT: Three novel tetranuclear vanadium(III) or (IV) complexes bridged by diphenyl phosphate or phosphate were prepared and their structures characterized by X-ray crystallography. The novel complexes are $[\{V(III)_2(\mu\text{-hpnbpda})\}_2\{\mu\text{-}(C_6H_5O)_2PO_2\}_2(\mu\text{-}O)_2]\cdot 6CH_3OH$ (**1**), $[\{V(III)_2(\mu\text{-tphpn})(\mu\text{-}\eta^3\text{-}HPO_4)\}_2(\mu\text{-}\eta^4\text{-}PO_4)](ClO_4)_3\cdot 4.5H_2O$ (**2**), and $[\{(V(IV)O)_2(\mu\text{-tphpn})\}_2(\mu\text{-}\eta^4\text{-}PO_4)](ClO_4)_3\cdot H_2O$ (**3**), where hpnbpda and tphpn are alkoxo-bridging dinucleating ligands. H_3hpnbpda represents 2-hydroxypropane-1,3-diamino-*N*,*N*′-bis(2-pyridylmethyl)-*N*,*N*′-diacetic acid, and Htphpn represents *N*,*N*,*N*′,*N*′-tetrakis(2-pyridylmethyl)-2-hydroxy-1,3-propanediamine. A dinuclear vanadium(IV) complex without a phosphate bridge, $[(VO)_2(\mu\text{-tphpn})(H_2O)_2](ClO_4)_3\cdot 2H_2O$ (**4**), was also prepared and structurally characterized for comparison. The vanadium(III) center in **1** adopts a hexacoordinate structure while that in **2** adopts a heptacoordinate structure. In **1**, the two dinuclear vanadium(III) units bridged by the alkoxo group of hpnbpda are further linked by two diphenylphosphato and two oxo groups, resulting in a dimer-of-dimers. In **2**, the two vanadium(III) units bridged by tphpn are further bridged by three phosphate ions with two different coordination modes. Complex **2** is oxidized in aerobic solution to yield complex **3**, in which two of the three phosphate groups in **2** are substituted by oxo groups.

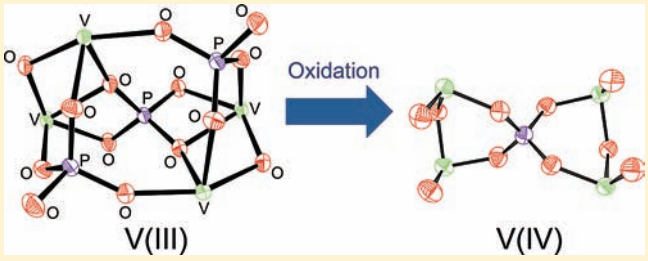

INTRODUCTION

Vanadium in biological systems has become an important area of research, and several review articles have been published focusing on the biological roles of vanadium.[1−9] Among the vanadium compounds in biological systems, vanadium in ascidians (also known as sea squirts or tunicates) has been the least characterized. Certain ascidians are known to accumulate vanadium to surprisingly high levels.[16] For example, *Ascidia gemmata* accumulates vanadium from seawater and stores it in its blood cells mainly as aqua complexes of vanadium(III) ($[V^{III}(H_2O)_6]^{3+}$ and $[V^{III}(HSO_4)(H_2O)_5]^{2+}$). The concentration of vanadium in *A. gemmata* reaches 350 mM,[10] 10^7-times higher than in seawater.[11] Vanadium in ascidians was discovered over 100 years ago by Henze,[16] and although some progress has been made in biochemically characterizing vanadium in ascidians,[12−15] the physiological role, as well as its relevance to biochemical reactions, remains unknown.

Consequently, we have studied the coordination chemistry of vanadium(III) to elucidate the biological role of vanadium in ascidians. We prepared vanadium(III) complexes containing sulfate, which coexists abundantly with vanadium(III) ions in ascidian vanadium-containing cells (vanadocytes),[17] and revealed their structures. We found that a didentate sulfate ion bridges two vanadium(III) centers together with an alkoxo-bridging dinucleating ligand, hpnbpda (H_3hpnbpda = 2-hydroxypropane-1,3-diamino-*N*,*N*′-bis(2-pyridylmethyl)-*N*,*N*′-diacetic acid) as a supporting ligand, yielding a heptacoordinate dinuclear vanadium(III) complex, $[\{V^{III}(H_2O)\}_2(\mu\text{-hpnbpda})(\mu\text{-}SO_4)(\mu\text{-}OH)]\cdot 5.25H_2O$, or a hexacoordinate tetranuclear vanadium(III) complex, $[V^{III}_4(\mu\text{-hpnbpda})_2(\mu\text{-}SO_4)_2(\mu\text{-}OH)_2]\cdot 12H_2O$. Thus, we developed new phosphate-vanadium(III) complexes to compare the properties of the sulfato and phosphato vanadium(III) complexes.

Phosphate and its esters are biological, inorganic species that are found ubiquitously in living organisms: cells typically contain 10 mM of inorganic phosphate.[18] Many studies have focused on the cleavage of phosphate esters activated by metal ions with regard to the activity of purple acid phosphatases (PAPs). PAPs are polyphosphate- and phosphate ester-cleaving enzymes containing a dinuclear metal unit bridged by a phosphate or phosphate ester,[19] which suggests that dinuclear complexes bridged by phosphate groups are an important motif in biological metal compounds.

Regarding the interaction of vanadium ions with phosphate, previous studies may be classified into two categories based on the oxidation state of vanadium. The first category includes studies related to the fact that $V(V)O_4^{3-}$ ions (vanadate) have a similar structure to the phosphate ion.[20−24] The second category involves studies based on the fact that vanadium(V)

Received: November 15, 2011
Published: April 9, 2012

   dx.doi.org/10.1021/ic2024617 | *Inorg. Chem.* 2012, 51, 5026−5036

Scheme 1. Various Coordination Modes of the Phosphate Ion[a]

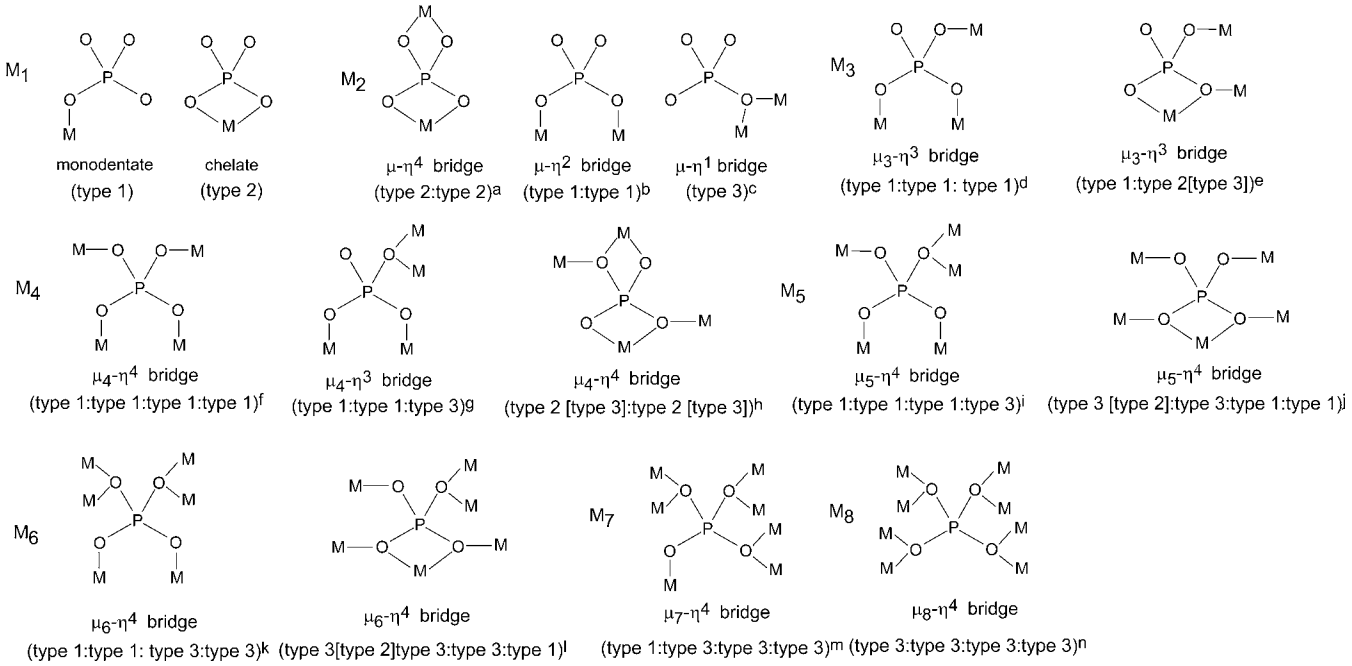

[a]a: ref 35; b: ref 36; c: ref 37; d: ref 38; e: ref 29; f: ref 39; g: ref 40; h: ref 41; i: ref 38; j: ref 40; k: ref 42; l: ref 43; m: ref 44; n: ref 45.

can be reduced to vanadium(IV) under physiological conditions, and further to vanadium(III) in some organisms, such as ascidians. Hence, investigating complexes of vanadium(IV) and (III) ions with phosphate ions is important. Numerous studies (mainly solution studies) have been performed on the interaction of oxovanadium(IV) species with inorganic phosphates and polyphosphate,[25] phosphate-esters, phosphonates and its derivatives,[26] organic compounds with phosphate groups,[27] and the phosphate groups of nucleotides.[25c,28] By contrast, solid-state structural studies using vanadium(III) species are limited to those published by Carrano's group from 1994 to 1997.[29−34]

Phosphate is considered a unique ligand from the standpoint of coordination stereochemistry since it can coordinate to a metal center with a variety of coordination modes. Some characteristic coordination modes are summarized in Scheme 1. In addition to simple monodentate or chelate coordination, phosphate ions frequently function as a bridging ligand with diverse coordination modes. Two (η^2), three (η^3), and even four (η^4) oxygen atoms of the phosphate ion can function as a bridging atom. Furthermore, one phosphate oxygen atom can bridge two or three metal centers. This type of coordination mode is rare in other biologically relevant inorganic ions, such as carbonate and sulfate, and may reflect the higher electron density of the phosphate oxygen atoms compared to carbonate and sulfate oxygen atoms.

In metalloenzymes, metal ions adopt the most suitable structure for the specific enzymatic reaction, but the structure of the active centers of metalloenzymes often resembles those of other enzymes. For example, the dinuclear unit bridged by carboxylate groups and oxo (or hydroxo) groups has been found in a wide range of metalloenzymes such as hemerythrin, ribonucleotide reductase, methane monooxygenase, and the PAPs. In addition, considerable variability in metal ion affinity exists within the metalloenzymes. For example, some dinuclear metallohydrolases have a high affinity for their native metal ions, while others have readily exchangeable metal ions.[46] More specifically, a wide variety of metal ions can be used to activate metalloenzymes for phosphate hydrolysis: Mg(II), Ca(II), Zn(II), Co(II), Co(III), Fe(II), Fe(III), Mn(II), and Cd(II) are all naturally used or are good substitutions.[47] Another example is a vanadium-dependent nitrogenase, in which a molybdenum atom is replaced by a vanadium atom.[48] On the basis of the above facts, we believe that the possibility exists that the vanadium(III) ion in ascidians, adopting a structure similar to other known metalloenzymes, plays an important role in biological reactions and replaces other biologically common metal ions, such as Fe(III). Consequently, investigating the properties of the vanadium(III) complex, which has a structure that mimics known metalloenzymes, is important for characterizing probable vanadium enzymes in ascidians.

We examined the coordination mode of phosphate to vanadium. We used dinucleating ligands with an alkoxo bridging group, hpnbpda and tphpn (Htphpn = *N,N,N′,N′*-tetrakis(2-pyridylmethyl)-2-hydroxy-1,3-propanediamine), as a supporting ligand to stabilize the dinuclear unit of vanadium(III) ions. Although a rigid tridentate capping ligand, such as tacn (1,4,7-triazacyclononane)[47,49,50] and hydrotris(pyrazolyl)borate,[30−32,34] are often used to construct model complexes of metalloenzymes, we selected the above flexible ligands since we also explored possible conformational changes of the ligand induced by coordination of the phosphate. Hpnbpda was used to construct dinuclear Zn(II) complexes as a model of RNase.[51] Other dinucleating ligands with an alkoxo bridging functionality (Scheme 2) have been used to construct a structural and functional model of several metalloenzymes: HBPCINOL,[52] Hbpmp,[53] and HBPBPMP and its derivative.[54] In this report, we discuss the preparation, structure, and properties of new vanadium(III) and (IV) complexes bridged by a phosphate group.

dx.doi.org/10.1021/ic2024617 | *Inorg. Chem.* 2012, 51, 5026−5036

Scheme 2. Alkoxo-Bridging Dinucleating Ligands

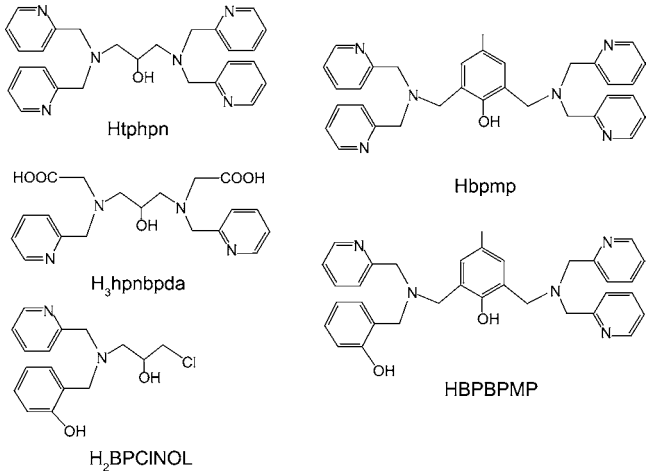

EXPERIMENTAL SECTION

Materials. Alkoxo-bridging dinucleating ligands, H_3hpnbpda·HBr·$3H_2O$ and Htphpn·$4HClO_4$, were prepared as previously described.[55] All other reagents were commercially available and used without further purification.

Preparation of Complexes. All manipulation was performed under an argon atmosphere using standard Schlenk techniques or in a nitrogen-filled drybox.

[{V(III)$_2$(μ-hpnbpda)}$_2${μ-(C$_6$H$_5$O)$_2$PO$_2$}$_2$(μ-O)$_2$]·6CH$_3$OH (**1**). H_3hpnbpda·HBr·$3H_2O$ (0.52 g: 1 mmol) was neutralized by lithium hydroxide monohydrate (0.21 g: 5 mmol) in methanol (10 mL). Diphenyl phosphoric acid (0.25 g: 1 mmol) was then added to this solution. A methanolic solution (10 mL) of vanadium(III) chloride (0.31 g: 2 mmol) was added to the above mixture, forming a dark brown solution. A small amount of pale green powder was deposited when left standing at ambient temperature. This impurity was discarded by filtration, and the filtrate was again allowed to stand at room temperature. The desired complex crystallized as dark brown plates. The crystals were collected by filtration, then washed with methanol, air-dried, and kept under an argon atmosphere (yield: 0.23 g, 27%). Anal. Calcd for $C_{68}H_{86}N_8O_{26}P_2V_4$: C, 48.12; H, 5.10; N, 6.60%. Found: C, 48.06; H, 5.22; N, 6.59%. Selected IR bands/cm^{-1} (Supporting Information, Figure S1): 1663 (ν_{as}(CO$_2$)), 1342 (ν_s(CO$_2$)), 1486, 1446, 1037, 1202, 954, 933, 757, 689.

[{V(III)$_2$(μ-tphpn)(μ-η^3-HPO$_4$)}$_2$(μ-η^4-PO$_4$)](ClO$_4$)$_3$·4.5H$_2$O (**2**). Htphpn·$4HClO_4$ (0.85 g: 1 mmol) was dissolved in 20 mL of water, and its perchloric acid moieties were neutralized by sodium hydroxide (0.16 g: 4 mmol). Na_2HPO_4 (0.21 g: 1.5 mmol) was dissolved in water/ethanol (1:1) solution (20 mL). To an aqueous solution (100 mL) of vanadium(III) chloride (0.32 g: 2 mmol), the tphpn solution was added, followed by the addition of the phosphate solution, resulting in a greenish brown suspension. This suspension was allowed to stand at ambient temperature, resulting in a purple solution. The solution turned orange after a few days, and reddish orange crystals were deposited. The crystals were filtered, washed with cold water, and air-dried (yield: 0.56 g, 64%). Anal. Calcd for $C_{54}H_{67}N_{12}Cl_3O_{29.5}P_3V_4$: C, 36.49; H, 3.91; N, 9.46%. Found: C, 36.87; H, 3.84; N, 9.55%. Selected IR bands/cm^{-1} (Supporting Information, Figure S2): 1611, 1574, 1484, 1447, 1091.

[{(V(IV)O)$_2$(μ-tphpn)}$_2$(μ-η^4-PO$_4$)](ClO$_4$)$_3$·H$_2$O (**3**). The orange reaction solution of **2** was exposed to air, resulting in a greenish-blue solution. The solution was transferred to a sealed flask and allowed to stand at 50 °C in a water bath. After 2 weeks, the deposited blue plate crystals were collected by filtration, washed with water, and air-dried (yield: 0.15 g, 37%). Anal. Calcd for $C_{54}H_{64}N_{12}Cl_3O_{25}PV_4$: C, 40.89; H, 3.81; N, 10.60%. Found: C, 40.84; H, 3.87; N, 10.58%. Selected IR bands/cm^{-1} (Supporting Information, Figure S3): 1609, 1089, 1056, 1024, 973, 917, 773, 625.

[(VO)$_2$(μ-tphpn)(H$_2$O)$_2$](ClO$_4$)$_3$·2H$_2$O (**4**). Htphpn·$4HClO_4$ (0.85 g: 1 mmol) was dissolved in 20 mL of water/EtOH (3:1), and its perchloric acid moieties were neutralized by 4 mL of 1 N NaOH solution, which yielded a yellow solution. An aqueous solution (50 mL) of VCl_3 (0.16 g: 1.0 mmol) was mixed with the yellow solution, resulting in an orange-brown solution. The solution was kept standing in the open air. The color of the solution changed to greenish-blue after a few days. The solution was concentrated to 20 mL. Blue columnar crystals were deposited the next day at ambient temperature. The crystals were harvested by filtration, washed with cold water, and air-dried (yield: 0.15 g, 31%). The above yield is that for obtaining good crystals. If good-quality crystals are not necessary, the yields could be improved to 51% by concentrating the solution further. Anal. Calcd for $C_{27}H_{34}N_6ClO_{13}PV_2$: C, 33.89; H, 3.79; N, 8.79%. Found: C, 33.82; H, 3.94; N, 8.81%. Selected IR bands/cm^{-1} (Supporting Information, Figure S4): 1615, 1109, 1033, 979, 910, 763, 625.

Caution! *Perchlorate salts are potentially explosive, especially in the presence of organic ligands. Therefore, the perchlorate complexes must be handled with care and prepared only in small amounts.*

Measurements. UV−vis absorption and diffuse reflectance spectra were measured using a Shimadzu UV-3100PC, JASCO V-650, and JASCO V-570 spectrophotometers, respectively. Infrared spectra were obtained with JASCO FT/IR-6100. Raman spectra were recorded on a JASCO NRS-7100 laser Raman spectrophotometer with excitation by a green laser line at 532 nm.

X-ray Structure Determination. A crystal was mounted on a glass fiber, coated with epoxy as a precaution against solvent loss, and centered on a Rigaku Mercury CCD (complex **1**), Rigaku variMaxRAPID-DW/NAT (complexes **2** and **4**), or Rigaku AFC-7R (complex **3**) using graphite monochromated Mo−Kα radiation (Complexes **1**, **2**, and **3**) or Cu- Kα (Complex **4**) radiation loaded by the confocal mirror, at −80 °C (complex **1**), −100 °C (complexes **2** and **4**), or −73 °C (complex **3**). Data reduction and the application of Lorentz polarization, the linear decay correction, and the empirical absorption correction were performed. The structures were solved by direct methods (DIRDIF99[56] for complex **1** and SHELX97[57] for complexes **2**, **3**, and **4**) and conventional difference Fourier technique, SHELX97. Non-hydrogen atoms were refined anisotropically, and hydrogen atoms were refined using the riding model. For complex **1**, the positions of the solvated methanol molecules could not be determined because of severe disorder in the unit cell. Experimental data for this study are listed in Table 1.

THEORETICAL CALCULATIONS

Electronic structure calculations for complex **1** were performed using the X-ray structure at a density functional theory (DFT) level with Gaussian 09.[58] A hybrid density functional of PBE1PBE[59] was used for the DFT calculations. The basis functions used were Dunning-Hay's split-valence double-ζ for C, H, N, and O atoms (D95) and the Hay-Wadt double-ζ with a Los Alamos relativistic effective core potential for the V atom (LANL2DZ).[60] The molecular orbitals were drawn using MOLEKEL.[61]

RESULTS AND DISCUSSION

Preparation of Vanadium(III) Complexes with Phosphate. We attempted to crystallize the vanadium(III) complex with phosphate using various combinations of vanadium(III) salts (VX_3: X = Cl^-, Br^-, and ClO_4^-), alkoxo-bridging dinucleating ligands (dpot = 2-oxo-1,3-diaminopropane-*N*,*N*,*N*′,*N*′-tetraacetate, hpnbpda, and tphpn), and phosphates (phosphate, monophenyl phosphate, and diphenyl phosphate). We also adjusted the acidity of the reaction solution to find an appropriate condition for formation and crystallization of the desired complex. We successfully isolated crystals of two new phosphato vanadium(III) complexes, for which the structure and properties will be described in the following sections.

dx.doi.org/10.1021/ic2024617 | Inorg. Chem. 2012, 51, 5026−5036

Table 1. Crystallographic Data

	1	2	3	4
formula	$C_{68}H_{86}N_8O_{26}P_2V_4$	$C_{54}H_{69}Cl_3N_{12}O_{30.5}P_3V_4$	$C_{54}H_{60}Cl_3N_{12}O_{23}PV_4$	$C_{27}H_{37}Cl_3N_6O_{19}V_2$
formula wt/g	1697.18	1770.18	1586.22	957.86
crystal size/mm	0.60 × 0.35 × 0.15	0.21 × 0.17 × 0.12	0.49 × 0.32 × 0.10	0.15 × 0.10 × 0.10
crystal system	triclinic	monoclinic	monoclinic	orthorhombic
space group	$P\bar{1}$ (No. 2)	$P2_1/a$ (No. 14)	$P2_1/n$ (No. 14)	$Pbca$ (No. 61)
a/Å	12.1064(2)	13.1574(3)	14.831(5)	16.7141(3)
b/Å	13.3772(2)	27.0473(5)	28.578(7)	11.0145(2)
c/Å	15.8191(2)	20.0567(4)	15.379(8)	40.7590(8)
α/deg	69.701(8)			
β/deg	68.285(8)	98.2019(7)	94.91(4)	
γ/deg	63.868(7)			
Z	1	4	4	8
V/Å^3	2084.2(1)	7064.6(3)	6494(5)	7503.6(3)
D_{calcd}/g cm^{-3}	1.354	1.406	1.659	1.696
λ/Å	0.71070 (Mo $K\alpha$)	0.71070 (Mo $K\alpha$)	0.71070 (Mo $K\alpha$)	1.54187 (Cu $K\alpha$)
$\alpha\mu$/cm^{-1}	5.49 (Mo $K\alpha$)	7.67 (Mo $K\alpha$)	8.0 (Mo $K\alpha$)	6.94 (Cu $K\alpha$)
$2\theta_{max}$/deg	55.0	54.9	60.0	136.5
temp/K	193	173	200	173
reflections				
total	33614	68957	19978	82545
unique	9379	16127	18937	6863
observed	7319 ($I > 3\sigma(I)$)	11732 ($I > 2\sigma(I)$)	8554 ($I > 2\sigma(I)$)	6863 ($I > 2\sigma(I)$)
F(000)	882	3412	3320	3920
no. of variables	512	1034	955	530
R^a (R_w)^b	0.089 (0.126)	0.0442 (0.1177)	0.0742 (0.1864)	0.0661 (0.1712)

$^aR = \sum||F_o| - |F_c||/\sum|F_o|$. $^bR_w = [\sum w(|F_o| - |F_c|)^2/\sum w|F_o|^2]^{1/2}$.

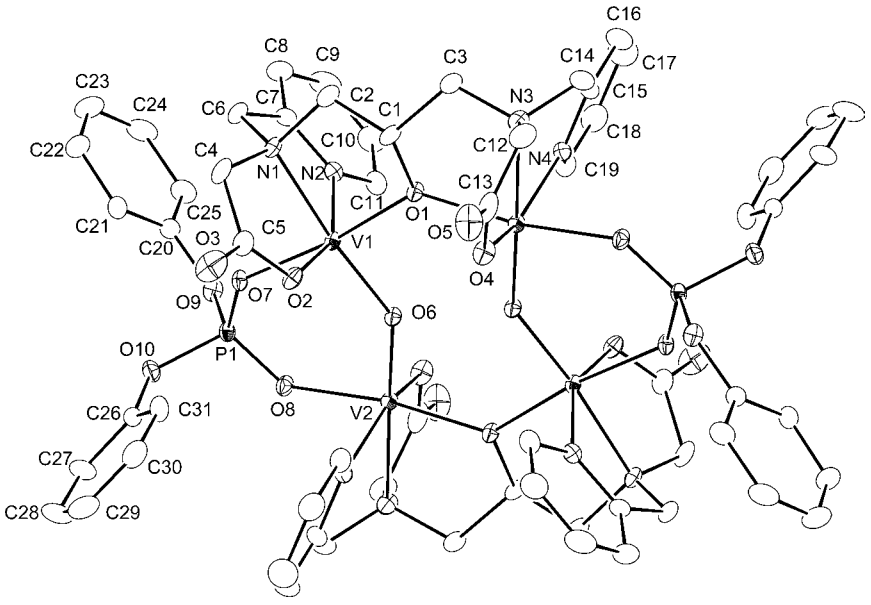

Figure 1. Perspective view of complex **1**.

Since the rate of crystallization of complex **1** is very slow, a better yield would be expected by letting the reaction solution stand for a long period. However, we found that when the solution was kept standing for a long period, vanadium(III) was oxidized to (IV), probably because of residual dioxygen in the reaction solution or the influx of dioxygen into the reaction vessel through small gaps. Therefore, we collected the crystals of complex **1** before the oxidation occurred, which resulted in the low yield.

Structure of Complex 1. The structure of complex **1** was determined by X-ray crystal analysis. Complex **1** effloresces since its methanol solvate tends to be removed from the crystals at ambient temperature. Thus, collection of the X-ray diffraction data was performed at −80 °C. Disorder of the methanol molecules resulted in a rather limited R-index (0.089), but the molecular structure of the complex is considered accurate.

Complex **1** was a centrosymmetric tetranuclear vanadium(III) complex. This structure is very similar to the corresponding sulfato complex, $[V^{III}_4(\mu\text{-hpnbpda})(\mu\text{-OH})_2(\mu\text{-SO}_4)_2]$, obtained in a previous study.[17] A perspective view of complex **1** is shown in Figure 1, and selected bond distances and angles are summarized

dx.doi.org/10.1021/ic2024617 | Inorg. Chem. 2012, 51, 5026−5036

in Table 2. Two dinuclear vanadium(III) units bridged by the alkoxo group of the hpnbpda ligand are further linked by two oxo and two diphenylphosphato bridging groups, resulting in a tetranuclear structure (dimer-of-dimers). The oxygen atom in the oxo bridging group is thought to come from a water molecule in methanol since the methanol used was not dry. The diphenylphosphate bridges two vanadium(III) centers in a μ_2-η^2 fashion (type 1:type 1 in Scheme 1), as found in dinuclear $[LVCl\{\mu\text{-}(PhO)_2PO_2\}]_2$ (**a**)[31] and trinuclear complexes, $[LV(\mu\text{-}(PhO)_2PO_2)_3\text{-}V\text{-}(\mu\text{-}(PhO)_2PO_2)_3VL]PF_6$ (**b**),[32] $[LV(\mu\text{-}(PhO)_2PO_2)_2(\mu\text{-}OH)\text{-}V\text{-}(\mu\text{-}(PhO)_2PO_2)_2(\mu\text{-}OH)VL]ClO_4$ (**c**),[32] and its heterometallic analogues,[34] where L = hydrotris(pyrazolyl)borate. Two vanadium(III) centers are doubly bridged by two diphenylphosphato groups in complex **a**, triply bridged by three diphenylphosphato groups in complex **b**, and triply bridged by two diphenylphosphato groups and one hydroxo group in complex **c**. As a result, these complexes form eight-membered V(OPO)V(OPO) ring(s). By contrast, in the dinuclear moiety in complex **1**, two vanadium(III) centers are bridged doubly by a diphenylphosphato and an oxo group, yielding only one six-membered V(OPO)V(O) ring. These differences in the bridging mode reflect differences in the V···V distances. The V···V distance in complex **1** is 3.578(2)Å, which is considerably shorter than those in complexes **a** (5.210(2) Å) and **b** (4.692(2) Å), in which two vanadium atoms are bridged solely by the diphenylphosphate groups, but comparable to complex **c** (3.613 Å), which includes two six-membered V(OPO)V(OH) rings in addition to one eight-membered V(OPO)V(OPO) ring.

Table 2. Selected Bond Distances (Å) and Angles (deg) for $[\{V(III)_2(hpnbpda)\}_2\{(C_6H_5O)_2PO_2\}_2(\mu\text{-}O)_2]\cdot 6CH_3OH$ (1)

V1—O1	2.018(5)	V2—O1[a]	2.033(3)
V1—O2	1.947(4)	V2—O4[a]	1.958(4)
V1—O6	1.910(4)	V2—O6	1.884(5)
V1—O7	2.073(5)	V2—O8	2.054(4)
V1—N1	2.159(5)	V2—N3[a]	2.160(8)
V1—N2	2.132(4)	V2—N4[a]	2.129(5)
V1···V2	3.578(2)	V1···V2[a]	3.724(2)
O1—V1—O2	92.5(2)	O1[a]—V2—O4[a]	91.49(16)
O1—V1—O6	92.8(2)	O1[a]—V2—O6	93.6(2)
O1—V1—O7	172.8(2)	O1[a]—V2—O8	170.9(2)
O1—V1—N1	83.3(2)	O1[a]—V2—N3[a]	83.2(2)
O1—V1—N2	95.9(2)	O1[a]—V2—N4[a]	90.95(17)
O2—V1—O6	104.9(2)	O4[a]—V2—O6	105.9(2)
O2—V1—O7	86.0(2)	O4[a]—V2—O8	88.42(17)
O2—V1—N1	79.9(2)	O4[a]—V2—N3[a]	79.2(2)
O2—V1—N2	154.0(2)	O4[a]—V2—N4[a]	154.5(3)
O6—V1—O7	94.4(2)	O6—V2—O8	95.1(2)
O6—V1—N1	174.0(2)	O6—V2—N3[a]	174.17(19)
O6—V1—N2	99.3(2)	O6—V2—N4[a]	99.3(2)
O7—V1—N1	89.6(2)	O8—V2—N3[a]	87.8(2)
O7—V1—N2	82.6(2)	O8—V2—N4[a]	85.28(18)
N1—V1—N2	76.7(2)	N3[a]—V2—N4[a]	75.9(2)
O6—V2—O8	95.1(2)		

[a]Symmetry code, 1−*x*, 1−*y*, −*z*.

The terminal tridentate moiety of hpnbpda can coordinate to a metal center in either a facial or a meridional fashion. The hpnbpda ligand in **1** adopts a meridional coordination mode despite the fact that facial coordination is more relaxed. This meridional coordination results in a large distortion in the octahedron around V(III), which is represented by small *trans* angles of O2−V1−N2 (154.0(2)°) and O4*−V2−N4* (154.5(3)°).

Notably, the bridging oxygen atoms are fully deprotonated oxo (O^{2-}) ligands in complex **1**, while they are hydroxo ligands in the corresponding sulfato complex. Since the sum of the negative charges including the additional bridging groups, that is, $(PhO)_2PO_2^- + O^{2-}$ and $SO_4^{2-} + OH^-$, is equal to 3 for both complexes, these complexes are both neutral.

Coordination bond distances and angles for complex **1** and for the sulfato complex are compared in Table 3. The corresponding coordination bond distances of both complexes are very similar (within 0.04 Å). The corresponding coordination bond angles are also similar, except for N_{py}−V−OP/OS and μ-O/OH−V−O_{carb}. The N_{py}−V−OP/OS angle of complex **1** is 8.5° smaller, while the μ-O/OH−V−O_{carb} angle is 19.2° larger, than the corresponding sulfato complex angles. The other angles are similar (within 2°−4°) between both complexes. The large differences in bond angles between the complexes may result from $\pi\cdots\pi$ stacking between the phenyl ring of the diphenylphosphate and the pyridine ring of the hpnbpda ligand in complex **1**, which is absent in the sulfato complex. The phenyl and pyridine rings are almost parallel (tilt

Table 3. Comparison of the Bond Distances and Angles between the Diphenylphosphato Complex (1) and Sulfato Complex[17]

bond distances[a]	phosphato	sulfato[b]	bond angles[a]	phosphato	sulfato[b]
V−N_{amino}	2.159(5)	2.175(3)	N_{amino}—V−N_{py}	76.7(2)	75.52(13)
V−N_{py}	2.132(4)	2.115(3)	N_{amino}—V−O_{alk}	83.3(2)	82.93(11)
V−O_{carb}	1.947(3)	1.986(2)	N_{amino}—V−O_{carb}	79.9(2)	78.57(12)
V−O_{alk}	2.018(5)	2.039(2)	N_{amino}—V−OP/OS	89.6(2)	92.49(12)
V—μ-O/OH	1.910(4)	1.880(2)	N_{py}—V−O_{alk}	95.9(2)	91.86(12)
V−OP/OS	2.073(5)	2.043(3)	O_{alk}—V−O_{carb}	92.5(2)	89.15(10)
V1···V2[1]	3.724(2)	3.7436(8)	O_{carb}—V−OP/OS	86.0(2)	85.74(12)
V1···V2[2]	3.578(2)	3.5320(7)	N_{py}—V−OP/OS	82.6(2)	91.13(13)
			μ-O/OH−V—O_{alk}	92.8(2)	92.49(10)
			μ-O/OH−V—O_{carb}	104.9(2)	85.74(12)
			μ-O/OH−V—OP/OS	94.4(2)	92.54(11)
			μ-O/OH−V—N_{py}	99.3(2)	98.47(12)
			V1—μ-O/OH−V2	141.2(3)	139.95(14)
			V1—O_{alk}—V2′	133.6(3)	133.25(3)

[a]N_{amino}, amino nitrogen; N_{py}, pyridyl nitrogen; O_{carb}, carboxylato oxygen; O_{alk}, alkoxo oxygen; V1···V2[1]: μ-alkoxo; V1···V2[2]: μ-O/OH, XO_4 (X = P or S). [b]The values are the average of the two independent moieties.

dx.doi.org/10.1021/ic2024617 | Inorg. Chem. 2012, 51, 5026−5036

angle of 5.6°) and separated by 3.9 Å, which indicates that the $\pi\cdots\pi$ interaction exists in complex **1**, although it is not significant. Consequently, the μ-O−V−O_{carb} angle in complex **1** would increase, resulting in a better overlap of the two rings, while the N_{py}−V−OP angle decreases because of attraction toward the phenyl ring.

UV−vis Spectrum of Complex 1. Figure 2 shows the absorption and diffuse reflectance spectra of complex **1**. The absorption spectrum was observed in methanol under anaerobic conditions. Since vanadium(III) complexes are substitution-labile, concern exists that the substitution of some ligands might occur in solution. Therefore, the absorption spectrum was compared with the diffuse reflectance spectrum in the solid state. The absorption spectrum of complex **1** (spectrum (a) in Figure 2) corresponds well to the diffuse

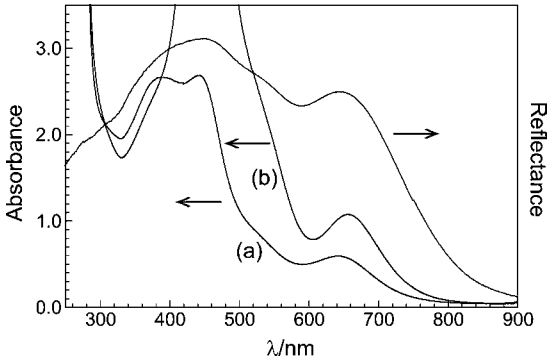

Figure 2. Absorption spectra of anaerobic methanol solution (3.4 mM/V(III)) (a) and of a solution with 1 equiv of LiOH added, and diffuse reflectance spectra of complex **1**.

reflectance spectrum in terms of the positions in the entire spectral region, indicating that a significant structural change such as dissociation of the ligands does not occur on dissolving in methanol. However, the protonation equilibria of the bridging oxo groups, as shown below, might occur in solution.

$$[(V_2L)(L')(\mu\text{-}O)_2] \underset{-H^+}{\overset{+H^+}{\rightleftharpoons}} [(V_2L)(L')(\mu\text{-}OH)(\mu\text{-}O)]^+ \underset{-H^+}{\overset{+H^+}{\rightleftharpoons}} [(V_2L)(L')(\mu\text{-}OH)_2]^{2+}$$
(**1**) (**1′**) (**1″**)

Complex **1** exhibits three distinct absorption bands at 399 (632 mol^{-1} dm^3 cm^{-1}/V(III)), 441 (574 mol^{-1} dm^3 cm^{-1}/V(III)), and 643 nm (136 mol^{-1} dm^3 cm^{-1}/V(III)), and a shoulder at about 550 nm (160 mol^{-1} dm^3 cm^{-1}/V(III)) in methanol. The sulfato analogue shows a band at 420 nm (295 mol^{-1} dm^3 cm^{-1}/V(III)), which was attributable to a charge transfer (CT) transition of the pyridyl groups to vanadium(III).[17] Vanadium(III) complexes with an oxo bridge to show a CT band due to the V−O−V moiety in the 420−540 nm region depending on the softness of the ancillary ligands.[61,62] Therefore, the 399 and 441 nm bands observed in complex **1** can be assigned to a pyridyl-CT and an oxo-CT transition, respectively. The sulfato analogue, which has a μ-hydroxo group instead of a μ-oxo group, shows only one band due to a pyridyl-CT transition at approximately 400 nm. The above assignment was confirmed by observing the absorption spectrum of the solution to which 1 equiv of LiOH was added (spectrum (b) in Figure 2). The intensity of the 441-nm band increased well beyond the observable range. This observation indicates that complex **1** exists at least as a partially protonated form in methanol, which would be converted to a deprotonated form by adding hydroxide, resulting in the increase in the intensity of the 441-nm band.

Although the lowest-energy transition bands around 643 and 550 nm are situated in the d−d transition region, the intensities of these bands appear too large for a pure d−d transition, for which the intensity is generally in the order of 10 for vanadium(III) complexes. To clarify the assignment of these visible bands, we performed theoretical calculations for complex **1** (Figure 3). The calculations for a hybrid density functional

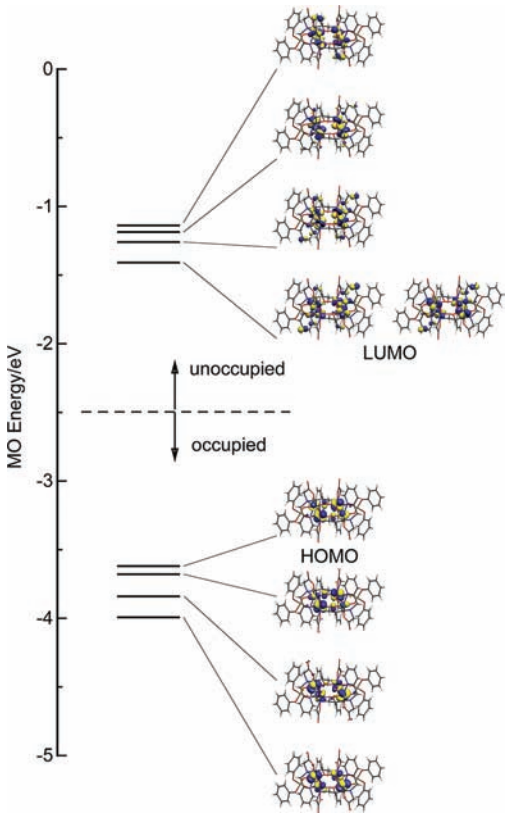

Figure 3. Orbital energies and frontier molecular orbitals of complex **1**.

theory (DFT) revealed that the singlet spin state had the lowest energy for the ground state, indicating that the predominant interaction between vanadium(III) ions bridged by oxo groups is antiferromagnetic. The frontier molecular orbitals involved in lower-energy electronic transitions are shown in Figure 3. The frontier occupied molecular orbitals (MOs) (HOMO∼HO-MO-3) are antibonding between 3d(V) and 2p(O) in the alkoxo and oxo groups, while the unoccupied MOs (LUMO∼LUMO+3) are composed of the 3d(V) and π^* orbitals of pyridyl moieties. Therefore, the lowest-energy transition bands in complex **1** are assignable to an admixture of d−d, ligand-to-metal charge transfer (LMCT), and metal-to-ligand charge-transfer (MLCT). These transitions could borrow intensity from allowed $d\pi \rightarrow \pi^*$ (MLCT) transitions and occur with moderate probability, that is, higher absorption coefficient compared with those for a pure d−d.

Structure of Complex 2. Complex **2** is a unique tetranuclear phosphato vanadium(III) complex. Two dinuclear units bridged by an alkoxo group of tphpn are further bridged by three phosphato ligands, resulting in a dimer-of-dimers. Perspective views (top and side) of complex **2** are shown in

dx.doi.org/10.1021/ic2024617 | Inorg. Chem. 2012, 51, 5026−5036

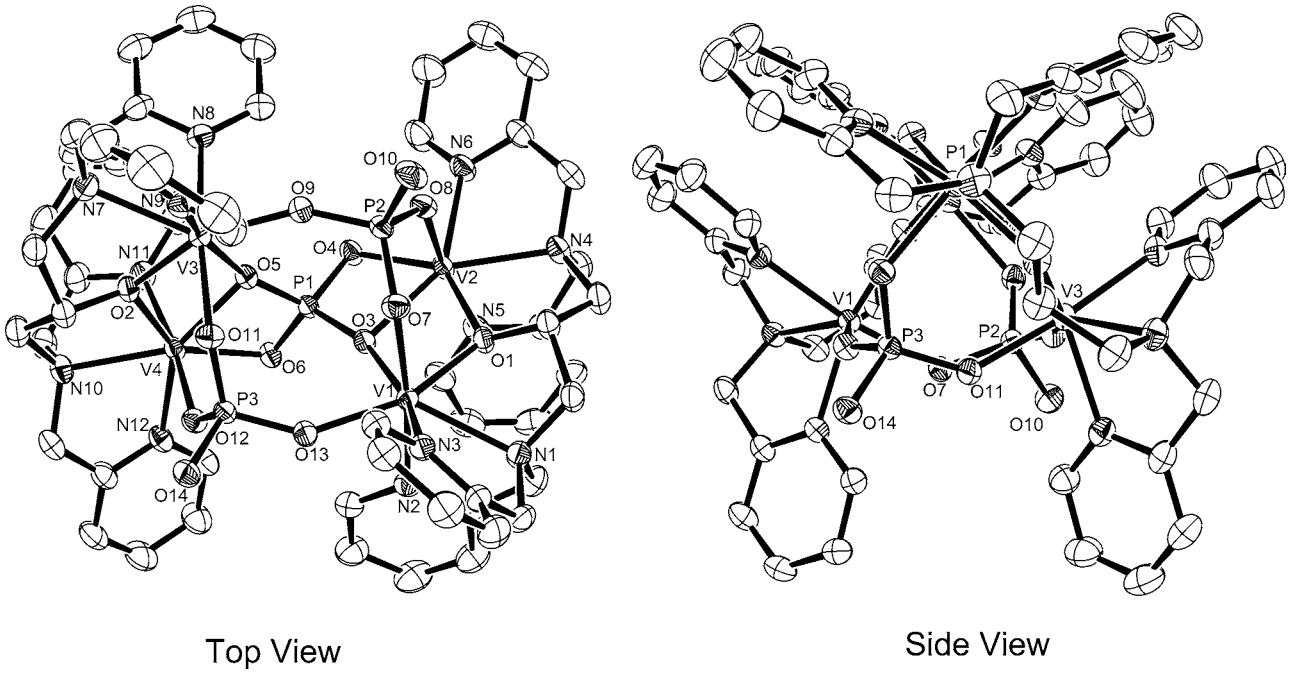

Figure 4. Perspective view of complex **2**.

Figure 4, and the core structure (which consists of three phosphate ligands) is shown in Supporting Information, Figure S5. As seen from the side view, a cavity exists in the center of the molecule. Selected bond distances and angles are summarized in Table 4.

The bridging phosphato ligands in this complex can be classified into two types: one coordinates to three vanadium(III) ions with a μ_3-η^3 mode (type 1:type 1:type 1 in Scheme 1). Considering a charge balance in complex **2**, this type of phosphate ion was assumed to be protonated (HPO_4^{2-}). The protonation of the μ_3-η^3 phosphate ion was confirmed by the increased P−O bond length (P2−O10: 1.590(3)Å and P3−O14: 1.5782(19)Å) compared to the other three PO bonds (1.51−1.54 Å), reflecting a localized single bond. These P−OH bond lengths agree with those found in $Rb[V(HPO_4)_2]$ (P−OH: 1.582 Å).[63] The other phosphate ion is fully deprotonated (PO_4^{3-}) and coordinates to four vanadium(III) centers with a unique coordination mode (μ_4-η^4: type 2[type 3]: type 2[type 3] in Scheme 1). Thus, O4 and O6 atoms singly coordinate to V2 and V4 atoms, respectively, while O3 and O5 atoms bridge V1 and V2 atoms, and V3 and V4 atoms, respectively. The bridging coordination of O3 and O5 atoms are confirmed by the fact that the two V−O bond lengths are similar and in the range of the coordination bond lengths; V1−O3: 2.0952(17) and V2−O3: 2.1524(18)Å, V3−O5: 2.0992(18) and V4−O5: 2.1280(19)Å. The coordination bond lengths of the singly coordinated oxygen atoms (V2−O4: 2.0792(19) and V4−O6: 2.080(2)Å) are shorter than those discussed above. This is consistent with the prediction that a single donation from one oxygen atom should be stronger than a double donation.

The terminal terdentate moiety of the tphpn ligand coordinates to the vanadium(III) center in a facial fashion, instead of the meridional coordination seen in complex **1**. The four vanadium(III) atoms adopt a heptacoordination, which also differs from the hexacoordination in complex **1**. The coordination bond lengths in complex **2** are slightly longer than the corresponding lengths in complex **1**, reflecting the increased

Table 4. Selected Bond Distances (Å) and Angles (deg) for $[\{V(III)_2(tphpn)(\mu_3\text{-}\eta^3\text{-}HPO_4)\}_2(\mu_4\text{-}\eta^4\text{-}PO_4)](ClO_4)_3\cdot 4.5H_2O$ (2)[a]

V1—O1	2.0232(18)	V1—O3	2.0952(17)
V1—O7	2.023(2)	V1—O13	2.012(2)
V1—N1	2.277(3)	V1—N2	2.187(3)
V1—N3	2.194(2)	V2—O1	2.0038(17)
V2—O3	2.1524(18)	V2—O4	2.0792(19)
V2—O8	2.0175(19)	V2—N4	2.240(3)
V2—N5	2.148(3)	V2—N6	2.187(3)
V1····V2	3.3653(6)	V2····V3	5.1368(6)
V3····V4	3.3800(6)	V4····V1	5.1639(6)
O1—V1—O3	69.63(7)	O1—V1—O7	83.16(8)
O1—V1—O13	156.72(8)	O1—V1—N1	68.61(8)
O1—V1—N2	96.06(8)	O1—V1—N3	122.48(8)
O3—V1—N7	88.00(8)	O3—V1—O13	87.37(7)
O3—V1—N1	128.47(8)	O3—V1—N2	82.98(8)
O3—V1—N3	160.22(8)	O7—V1—O13	92.81(8)
O7—V1—N1	115.18(8)	O7—V1—N2	170.61(8)
O7—V1—N3	78.81(8)	O13—V1—N1	132.62(8)
O13—V1—N2	84.21(8)	O13—V1—N3	78.72(8)
N1—V1—N2	72.88(9)	N1—V1—N3	71.01(8)
N2—V1—N3	109.20(8)	O1—V2—O3	68.83(7)
O1—V2—O4	135.93(8)	O1—V2—O8	86.66(8)
O1—V2—N4	74.24(8)	O1—V2—N5	88.79(8)
O1—V2—N6	143.30(9)	O3—V2—O4	67.32(7)
O3—V2—O8	90.61(8)	O3—V2—N4	142.08(8)
O3—V2—N5	93.42(8)	O3—V2—N6	145.65(9)
O4—V2—O8	97.92(8)	O4—V2—N4	147.42(8)
O4—V2—N5	89.57(8)	O4—V2—N6	80.41(8)
O8—V2—N4	95.60(9)	O8—V2—N5	172.41(9)
O8—V2—N6	82.18(8)	O8—V2—N4	77.30(9)
N4—V2—N6	72.24(9)		

[a]The data around V3 and V4 are omitted since they are similar to those around V1 and V2, respectively, although the four vanadium atoms are independent crystallographically.

dx.doi.org/10.1021/ic2024617 | Inorg. Chem. 2012, 51, 5026−5036

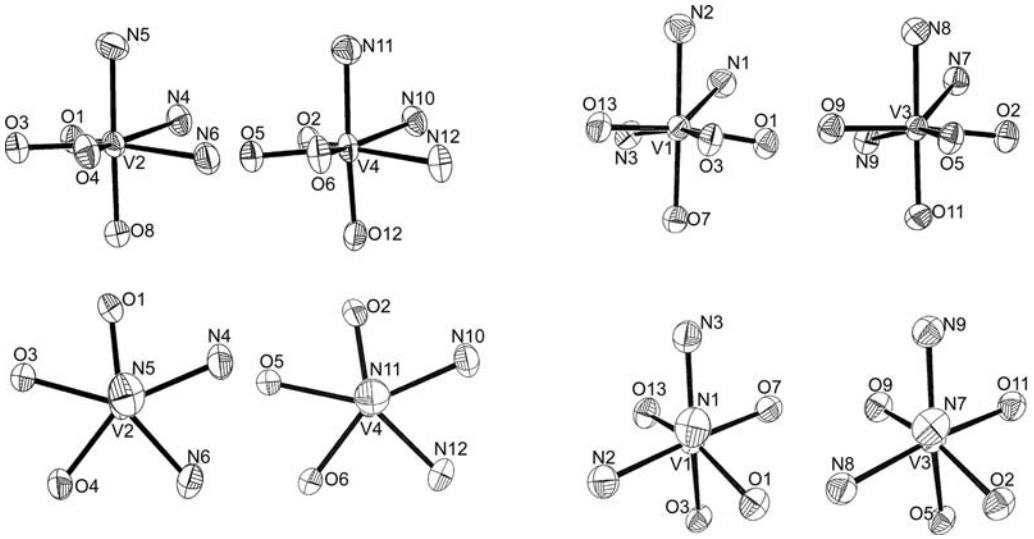

Figure 5. Coordination geometries around vanadium(III) ions in complex **2**.

coordination number. Since the phosphato vanadium(III) complexed with a rigid, tripodal capping ligand (hydrotris(pyrazolyl)borate) exclusively adopts a hexacoordination,[30,32,34] the heptacoordination in complex **2** results from a flexible coordination mode of the ancillary ligand.

Although heptacoordination is rare for first-row transition metal complexes, vanadium(III) often adopts a heptacoordination.[62] The ideal geometries for heptacoordination are pentagonal bipyramid, capped octahedron, and capped trigonal prism. The coordination geometries around the four vanadium(III) atoms are shown in Figure 5. From this figure, the coordination geometry around V2 and V4 can be best described as a pentagonal bipyramid in which a pyridyl nitrogen atom and a phosphate oxygen atom occupy the apical positions. On the other hand, the coordination geometry around V1 and V3 would be better described as a distorted, capped octahedron. The amino nitrogen atoms, N1 and N7, occupy the capping position. Note that the vanadium(III) atoms adopt two coordination geometries in one complex because the most stable arrangement of the coordinating atoms in the complex was established by flexibly changing the coordination geometries around the vanadium(III) ion. This flexibility is a distinct feature of the coordination chemistry of vanadium(III).

UV–vis Spectral Study of Complex 2. The absorption spectrum of complex **2** in water under anaerobic conditions was compared to the diffuse reflectance spectrum in the solid state in Figure 6. Reliable data could not be obtained in the longer wavelength region of the absorption spectrum because of the low solubility of complex **2**. The absorption spectrum corresponds well with the diffuse reflectance spectrum, except for the longer wavelength region, indicating that the structure found in the solid state was intact in water, as seen with complex **1**. The band at 830 nm (7 mol^{-1} dm^3 cm^{-1}/V(III)) can be assigned to a diagnostic band for heptacoordinated vanadium(III) complexes,[62] consistent with the X-ray structure. Other absorption bands were observed at 353 nm (769 mol^{-1} dm^3 cm^{-1}/V(III)), 500 nm (shoulder) (39 mol^{-1} dm^3 cm^{-1}/V(III)), and 580 nm (shoulder) (22 mol^{-1} dm^3 cm^{-1}/V(III)). The intense band at 353 nm is assignable to a CT transition of the pyridyl group of tphpn, as discussed for complex **1**, and the bands at 500 and 580 nm can be assigned to d–d transitions.

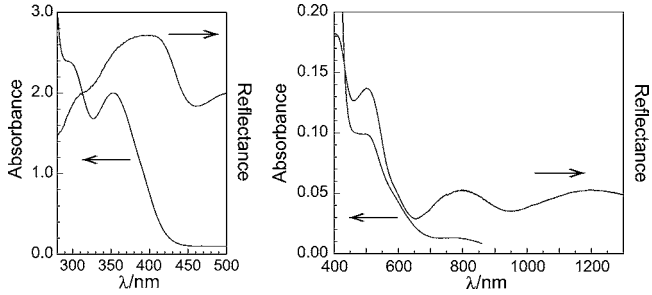

Figure 6. Absorption in anaerobic aqueous solution (2.8 mM/V(III)) and diffuse reflectance spectra of complex **2**: left side, 260–500 nm region; right side, spectrum magnified in the 400–1300 nm region.

Complex **2** is fairly stable in anaerobic solutions but slowly decomposes in aerobic solutions. Time-dependent absorption spectra of complex **2** under aerobic conditions are shown in Figure 7. The shoulder band around 500 nm decreases slowly

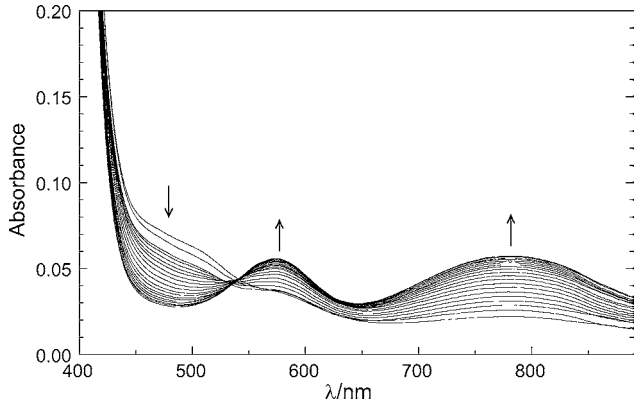

Figure 7. Time-dependent absorption spectra of complex **2** in aerobic aqueous solution (2.8 mM/V(III)) (every 5 h).

over time, while two new bands appear. After 12 h, an approximate isosbestic point was discerned at 530 nm, suggesting that the oxidation product of complex **2** is not a complex mixture, but a simple one with a dominant species. The final spectrum after 100 h is typical of oxovanadium(IV) complexes. This

dx.doi.org/10.1021/ic2024617 | Inorg. Chem. 2012, 51, 5026–5036

observation prompted us to isolate and characterize the oxidation product of complex **2**.

Structures of Complexes 3 and 4. Crystals of the oxidation product of complex **2** (complex **3**) were isolated, and the structure was determined by X-ray crystallography. The perspective view is shown in Figure 8, and bond lengths and

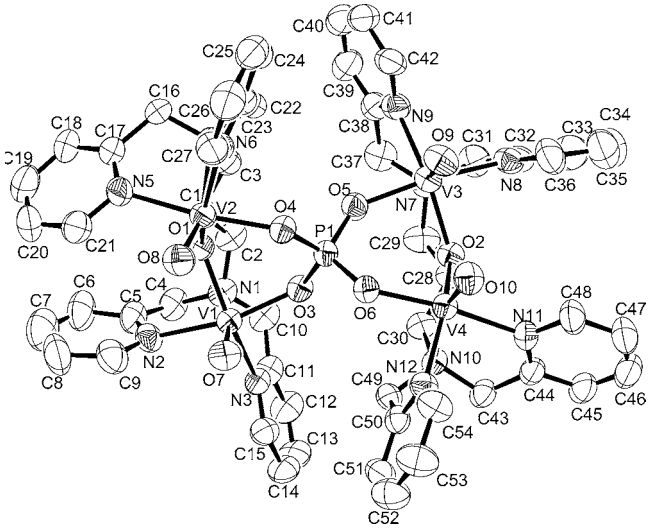

Figure 8. Perspective view of complex **3**.

angles are summarized in Table 5. Complex **3** is a tetranuclear oxovanadium(IV) complex, in which two dinuclear units bridged by an alkoxo group of tphpn is further bridged by a phosphate ion in a μ_4-η^4 fashion (type 1:type 1:type 1:type 1 in Scheme 1). On oxidation of complex **2**, the central phosphato group remained while the monoprotonated phosphato ligand, coordinated to the vanadium atom with a μ_3-η^3 fashion, was substituted by a ubiquitous oxo ligand of vanadyl(IV) species. The vanadium(IV) atom adopts a distorted octahedral geometry, and thus the coordination number was reduced from 7 to 6 upon oxidation. The amino nitrogen atoms of tphpn are situated in the *trans* position of the oxo group, resulting in comparatively long V−N bond lengths because of the *trans* influence of the oxo group.

While two of the four oxygen atoms of the central phosphate ion in complex **2** doubly coordinate to two vanadium(III) centers, each oxygen atom of the phosphate ion in complex **3** singly coordinates to one vanadium(IV) center. This suggests that the relative arrangement of the four vanadium atoms and the phosphate ion are changed upon oxidation. Figure 9 compares the relative arrangement between the V(III) and V(IV) complexes. While the tphpn ligand and the phosphate ion are arranged symmetrically in the V(IV) complex, the phosphate ion rotates with respect to the tphpn ligand in the V(III) complex, allowing one oxygen atom to coordinate two vanadium atoms. As a result, two four-membered rings are formed in complex **2**, instead of a six-membered ring seen in complex **3**. In addition, the OPO and VOV planes are almost coplanar in complex **2**, while the VOV plane is significantly bent from the OPO plane in complex **3**.

To determine if a conformational change in tphpn caused by the coordination of phosphate exists, the V(IV)O/tphpn complex without phosphate (complex **4**) was prepared and structurally characterized. Complex **4** is a dinuclear oxovanadium(IV) complex bridged by alkoxo oxygen of tphpn (Supporting

Table 5. Selected Bond Distances (Å) and Angles (deg) for $[\{V(IV)_2O_2(tphpn)\}_2(\mu_4\text{-}\eta^4\text{-}PO_4)](ClO_4)_3\cdot 3.5H_2O$ (3)[a]

V1—O1	1.990(4)	V1—O3	1.959(4)
V1—O7	1.604(4)	V1—N1	2.271(5)
V1—N2	2.156(5)	V1—N3	2.088(4)
V2—O1	2.002(4)	V2—O4	1.962(4)
V2—O8	1.595(4)	V2—N4	2.292(5)
V2—N5	2.165(5)	V2—N6	2.115(5)
V1····V2	3.405(2)	V2····V3	5.832(2)
V3····V4	3.429(1)	V1····V4	5.650(2)
O1—V1—O3	85.79(15)	O1—V1—O7	109.64(18)
O1—V1—N1	78.71(16)	O1—V1—N2	83.66(18)
O1—V1—N3	153.66(16)	O3—V1—O7	105.10(19)
O3—V1—N1	87.65(17)	O3—V1—N2	162.05(19)
O3—V1—N3	90.56(17)	O7—V1—N1	165.0(2)
O7—V1—N2	92.1(2)	O7—V1—N3	96.5(2)
N1—V1—N2	76.1(2)	N1—V1—N3	75.08(18)
N2—V1—N3	92.48(18)	O1—V2—O4	86.61(15)
O1—V2—O8	109.97(19)	O1—V2—N4	78.52(16)
O1—V2—N5	83.60(17)	O1—V2—N6	150.68(18)
O4—V2—O8	104.0(2)	O4—V2—N4	93.27(17)
O4—V2—N5	165.30(18)	O4—V2—N6	86.71(17)
O8—V2—N4	161.0(2)	O8—V2—N5	89.7(2)
O8—V2—N6	99.3(2)	N4—V2—N5	74.06(18)
N4—V2—N6	73.44(19)	N5—V2—N6	96.5119)

[a]The data around V3 and V4 are omitted since they are similar to those around V1 and V2, respectively, although the four vanadium atoms are independent crystallographically.

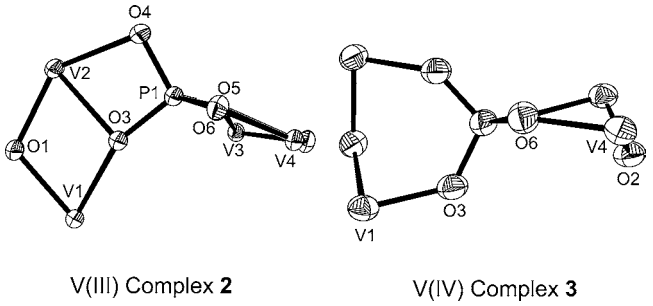

Figure 9. Comparison of the bridging modes of the phosphate ion in complexes **2** and **3**.

Information, Figure S7). Figure 10 shows the partial views of complexes **3** and **4** from the direction of the oxo groups. The plane constituted by the two pyridylmethyl groups and the central 2-oxo-1,3-propanediamine moiety of tphpn is rather flat in complex **4**, while in complex **3**, the corresponding plane is considerably bent because of the short PO···OP distance compared to the $H_2O\cdots OH_2$ distance in complex **4**. Since biological ligands such as proteins constituting metalloenzymes are structurally flexible, these results reveal useful information to understand the conformational changes in the biological metal complexes induced by coordination of phosphate.

Raman Spectra. Vibrational spectra have been used to determine the coordination mode of a simple ligand, such as sulfate or phosphate ions. However, distinguishing the infrared band due to sulfate or phosphate from other bands is difficult in many complexes, especially in those containing a large organic ligand. By contrast, the Raman band from symmetric stretching of the phosphate ion can be easily distinguished from the other bands since the high electron density of the PO bond makes it very intense. We observed the Raman spectra of the present

dx.doi.org/10.1021/ic2024617 | *Inorg. Chem.* 2012, 51, 5026−5036

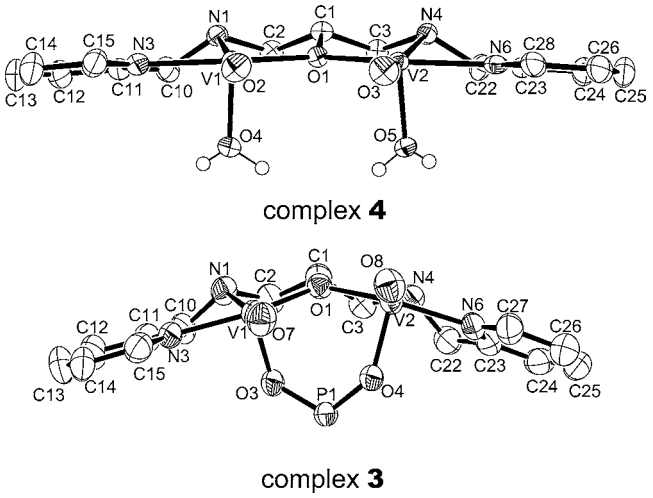

Figure 10. Comparison of the conformations of tphpn in complexes **3** and **4**.

phosphato complexes to obtain a criterion to determine whether the phosphate ion coordinates to a metal center or exists as a free ion. In the Raman spectra of simple salts (Na_3PO_4, Na_2HPO_4, and NaH_2PO_4), the symmetric stretching of PO_4 groups were observed at 939, 947, and 948 cm^{-1}, respectively. In complexes **2** and **3**, they were observed at 1003 and 1010 cm^{-1}, respectively (Supporting Information, Figures S9 and S10). Thus, the symmetric stretching of the PO_4 group shifts to a higher wavenumber by approximately 60 cm^{-1} when phosphate ions coordinate to a metal center. This higher wavenumber shift can be explained as follows. Coordination of the phosphate reduces the electron density on the oxygen atoms. The PO bond would then become stronger because of a reduced repulsion between the lone electron pair on the oxygen atom and the bonding electron pair of the PO bond. Although two types of phosphate ions exist in complex **2**, the symmetric PO stretching bands overlap significantly and only one band with asymmetric contours was observed. For complex **1** containing $(PhO)_2PO_2^-$ ions, no distinguished intense band was observed in the PO stretching region of the Raman spectrum (Supporting Information, Figure S8). Instead, the overtone of the asymmetric V(III)−O−V(III) stretching was observed as a very intense band at 1428 cm^{-1}, which is a distinguishing feature for oxo-bridged dinuclear vanadium(III) complexes.[64]

■ ASSOCIATED CONTENT

Supporting Information

Infrared spectra of complexes **1**∼**4** (Figures S1∼S4), the core structure of complex **2** (Figure S5), absorption and diffuse reflectance spectra of complex **3** (Figure S6), ORTEP drawings of complex **4** (Figure S7), and Raman spectra of complexes **1**∼**3** (Figures S8∼S10). This material is available free of charge via the Internet at http://pubs.acs.org. The CIF data have been deposited with the Cambridge Crystallographic Data Center (CCDC) [CCDC nos. 851803 (**1**), 871205 (**2**), 851801 (**3**), and 871203 (**4**)]. Copies of this information may be obtained free of charge from the director, CCDC, 12 Union Rd., Cambridge CB2 1EZ, U.K. (fax, +44-1223-336033; e-mail, deposit@ccdc.cam.ac.uk).

■ AUTHOR INFORMATION

Corresponding Author

*E-mail: kanamori@sci.u-toyama.ac.jp.

Notes

The authors declare no competing financial interest.

■ REFERENCES

(1) Michibata, H., Ed.; *Vanadium: Biochemical and Molecular Biological Approaches*; Springer: Dordrecht, The Netherlands, 2011.
(2) Rehder, D. *Bioinorganic Vanadium Chemistry*; Wiley: Chichester, U.K., 2008.
(3) Tracey, A.; Willsky, G. R.; Takeuchi, E. S. *Vanadium Chemistry, Biochemistry, Pharmacology and Practical Applications*; CRC Press: New York, 2007.
(4) Kustin, K.; Costa Pessoa, J.; Crans, D. C., Eds.; *Vanadium: The Versatile Metal*; ACS Symposium Series 974; American Chemical Society: Washington, DC, 2007.
(5) Lever, A. B. P. Ed.; *Coord. Chem. Rev.* **2003**; Vol. *237*.
(6) Tracey, A. S.; Crans, D. C., Eds.; *Vanadium Compounds: Chemistry, Biochemistry, and Therapeutic Applications*; ACS Symposium Series 711; American Chemical Society: Washington, DC, 1998.
(7) Nriagu, J. O., Ed.; *Vanadium in the Environment*; John Wiley: New York, 1998.
(8) Sigel, H., Sigel, A., Eds.; *Vanadium and Its Role in Life; Metal Ions in Biological Systems*; Marcel Dekker: New York, 1995; Vol. *31*.
(9) Chasteen, N. D., Ed.; *Vanadium in Biological Systems*; Kluwer Academic Publishers: Dordrecht, The Netherlands, 1990.
(10) Michibata, H.; Iwata, Y.; Hirata, J. *J. Exp. Zool.* **1991**, *257*, 306−313.
(11) Collier, R. W. *Nature* **1984**, *309*, 441−444.
(12) Ueki, T.; Adachi, T; Kawano, S.; Aoshima, M.; Yamaguchi, N.; Kanamori, K.; Michibata, H. *Biochim. Biophys. Acta* **2003**, *1626*, 43−50.
(13) Hamada, T.; Asanuma, M.; Ueki, T.; Hayashi, F.; Kobayashi, N.; Yokoyama, S.; Michibata, H.; Hirota, H. *J. Am. Chem. Soc.* **2005**, *127*, 4216−4222.
(14) Fukui, K.; Ueki, T.; Ohya, H.; Michibata, H. *J. Am. Chem. Soc.* **2003**, *125*, 6352−6353.
(15) Kawakami, N.; Ueki, T.; Amata, Y.; Kanamori, K.; Matsuo, K.; Gekko, K.; Michibata, H. *Biochim. Biophys. Acta* **2009**, *1794*, 674−679.
(16) Henze, M. *Hoppe−Seyler's Z. Physiol. Chem.* **1911**, *72*, 494−501.
(17) Kanamori, K.; Matsui, N.; Takagi, K.; Miyashita, Y.; Okamoto, K. *Bull. Chem. Soc. Jpn.* **2006**, *79*, 1881−1888.
(18) Willsky, G. R.; Goldfine, A. B.; Kostyniak, P. J. Pharmacology and Toxicology of Oxovanadium Species: Oxovanadium Pharmacology. In *Vanadium Compounds: Chemistry, Biochemistry, and Therapeutic Applications*; ACS Symposium Series 711, Chapter 22; Tracey, A. S., Crans, D. C., Eds.; American Chemical Society: Washington, DC, 1998; pp 278−296.
(19) Recent publications: (a) Mitic, N.; Noble, C. J.; Gahan, L. R.; Hanson, G. R.; Schenk, G. *J. Am. Chem. Soc.* **2009**, *131*, 8173−8179. (b) Gahan, L. R.; Smith, S. J.; Neves, A.; Schenk, G. *Eur. J. Inorg. Chem.* **2009**, 2745−2758. (c) Peralta, R. A.; Bortoluzzi, A. J.; de Souza, B.; Jovito, R.; Xavier, F. R.; Couto, R. A. A.; Casellato, A.; Nome, F.; Dick, A.; Gahan, L. R.; Schenk, G.; Hanson, G. R.; de Paula, F. C. S.; Pereira-Maia, E. C.; Machado, S.; de, P.; Servino, P. C.; Pich, C.; Bortolotto, T.; Terenzi, E. E.; Castellano, E. E.; Neves, A.; Rilley, M. J. *Inorg. Chem.* **2010**, *49*, 11421−11438.
(20) Cantley, L. C.; Josephson, L.; Warner, R.; Yanagisawa, M.; Lechene, C.; Guidotti, G. *J. Biol. Chem.* **1977**, *252*, 7421−7423.
(21) (a) Gresser, M. J.; Tracey, A. S.; Parkinson, K. M. *J. Am. Chem. Soc.* **1986**, *108*, 6229−6234. (b) Mendz, G. L. *Arch. Biochem. Biophys.* **1991**, *291*, 201−211. (c) Zhang, M.; Zhou, M.; Van Etten, R. L.; Stauffacher, C. V. *Biochemistry* **1997**, *36*, 15−23. (d) Plass, W. *Angew. Chem., Int. Ed.* **1999**, *38*, 909−912.
(22) Liochev, S.; Fridovich, I. *Arch. Biochem. Biophys.* **1990**, *279*, 1−7.
(23) Minasi, L. A.; Willsky, G. R. *J. Bacteriol.* **1991**, *173*, 834−841.
(24) Crans, D. C.; Marshman, R. W.; Nielsen, R.; Felty, I. *J. Org. Chem.* **1993**, *58*, 2244−2252.
(25) (a) Hasegawa, A.; Yamada, Y.; Miura, M. *Bull. Chem. Soc. Jpn.* **1969**, *42*, 846. (b) Hasegawa, A. *J. Chem. Phys.* **1971**, *55*, 3101−3104. (c) Cini, R.; Giorgi, G.; Laschi, F.; Sabat, M.; Sabatini, A.; Vacca, A. *J.*

Chem. Soc., Dalton Trans. **1989**, 575−580. (d) Buglyo, P.; Kiss, T.; Alberico, E.; Micera, G.; Dewaele, D. *J. Coord. Chem.* **1995**, *36*, 105−116. (e) Dikanov, S. A.; Liboiron, B. D.; Orvig, C. *J. Am. Chem. Soc.* **2002**, *124*, 2969−2978.
(26) (a) Sanna, D.; Micera, G.; Buglyo, P.; Kiss, T. *J. Chem. Soc., Dalton Trans.* **1996**, 1779. (b) Dean, N. S.; Bond, M. R.; O'Connor, C. J.; Carrano, C. J. *Inorg. Chem.* **1996**, *35*, 7643−7648. (c) Chang, Y. D.; Salta, J.; Zubieta, J. *Angew. Chem., Int. Ed. Engl.* **1994**, *106*, 347−350.
(27) Crans, D. C.; Anderson, F. J. O. P.; Miller, S. M. *Inorg. Chem.* **1998**, *37*, 6645−6655.
(28) (a) Woltermann, G. M.; Scott, R. A.; Haight, G. P. *J. Am. Chem. Soc.* **1974**, *96*, 7569. (b) Sakurai, H.; Goda, T.; Shimomura, S. *Biochem. Biophys. Res. Commun.* **1982**, *108*, 474−478. (c) Urretavizcaya, G.; Baran, E. J. *Z. Naturforsch.* **1987**, *42*, 1537−1542. (d) Etcheverry, S. B.; Ferrer, E. G.; Baran, E. J. *Z. Naturforsch.* **1989**, *44*, 1355−1358. (e) Williams, P. A. M.; Baran, E. J. *J. Inorg. Biochem.* **1992**, *48*, 15−19. (f) Mustafi, D.; Telser, J.; Makinen, M. W. *J. Am. Chem. Soc.* **1992**, *114*, 6219−6226. (g) Jiang, F. S.; Makinen, M. W. *Inorg. Chem.* **1995**, *34*, 1736−1744. (h) Alberico, E.; Dewaele, D.; Kiss, T.; Micera, G. *J. Chem. Soc., Dalton Trans.* **1995**, 425−430. (i) Buy, C.; Matsui, S.; Andrianambininstoa, S.; Sigalat, C.; Girault, G.; Zimmermann, J−L. *Biochemistry* **1996**, *35*, 14281−14293. (j) Petersen, J.; Fisher, K.; Mitchell, C. J.; Lowe, D. J. *Biochemistry* **2002**, *41*, 13253−13263.
(29) Mokry, L. M.; Thompson, J.; Bond, M. R.; Otieno, T.; Mohan, M.; Carrano, C. J. *Inorg. Chem.* **1994**, *33*, 2705−2706.
(30) Otieno, T.; Mokry, L. M.; Bond, M. R.; Carrano, C. J.; Dean, N. S. *Inorg. Chem.* **1996**, *35*, 850−856.
(31) Dean, N. S.; Mokry, L. M.; Bond, M. R.; O'Connor, C. J.; Carrano, C. J. *Inorg. Chem.* **1996**, *35*, 2818−2825.
(32) Dean, N. S.; Mokry, L. M.; Bond, M. R.; O'Connor, C. J.; Carrano, C. J. *Inorg. Chem.* **1996**, *35*, 3541−3547.
(33) Otieno, T.; Bond, M. R.; Mokry, L. M.; Walter, R. B.; Carrano, C. J. *Chem. Commun.* **1996**, 37−38.
(34) Dean, N .S.; Mokry, L. M.; Bond, M. R.; Mohan, M.; Otieno, T.; O'Connor, C. J.; Spartalian, K.; Carrano, C. J. *Inorg. Chem.* **1997**, *36*, 1424−1430.
(35) Connolly, J. A.; Banaszczyk, M.; Hynes, R. C.; Chin, J. *Inorg. Chem.* **1994**, *33*, 665−669.
(36) Zima, V.; Lii, K.-H. *J. Chem. Soc., Dalton Trans.* **1998**, 4109−4112.
(37) Lu, A.; Li, N.; Ma, Y.; Song, H.; Li, D.; Guan, N.; Wang, H.; Xiang, S. *Cryst. Growth Res.* **2008**, *8*, 2377−2383.
(38) Chang, W.-K.; Wur, C.-S.; Wang, S.-L.; Chiang, R.-K. *Inorg. Chem.* **2006**, *45*, 6622−6627.
(39) Shi, L.; Li, J.; Yu, J.; Li, Y.; Ding, H.; Xu, R. *Inorg. Chem.* **2004**, *43*, 2703−2707.
(40) Choudhury, A.; Neeraj, S.; Natarajan, S.; Rao, C. N. R. *Angew. Chem., Int. Ed.* **2000**, *39*, 3091−3093.
(41) Paul, R. L.; Amoroso, A. J.; Jones, P. L.; Couchman, S. M.; Reeves, R.; Rees, L. H.; Jeffery, J. C.; McCleverty, J. A.; Ward, M. D. *J. Chem. Soc., Dalton Trans.* **1999**, *10*, 1563−1568.
(42) Uchida, S.; Kawamoto, R.; Akatsuka, T.; Hikichi, S.; Mizuno, N. *Chem. Mater.* **2005**, *17*, 1367−1375.
(43) Lethbridge, Z. A. D.; Lightfoot, P. *J. Solid State Chem.* **1999**, *143*, 58−61.
(44) Xu, X.-X.; Zhang, X.; Liu, X.-X.; Sun, T.; Wang, Y.-H. *Transition Met. Chem.* **2009**, *34*, 571−577.
(45) Ritchie, C.; Li, F.; Pradeep, C. P.; Long, D.-L.; Xu, L.; Cronin, L. *Dalton Trans.* **2009**, 6483−6486.
(46) Wilcox, D. E. *Chem. Rev.* **1996**, *96*, 2435−2458.
(47) Williams, N. H.; Cheung, W.; Chin, J. *J. Am. Chem. Soc.* **1998**, *120*, 8079−8087.
(48) Eady, R. R. Vanadium Nitrogenases in Azotobacter. In *Vanadium in the Environment*; Nriagu, J. O., Ed.; John Wiley: New York, 1995; Chapter 11, pp 363−405.
(49) Hamphry, T.; Forconi, M.; Williams, H.; Hengge, A. C. *J. Am. Chem. Soc.* **2002**, *124*, 14860−14861.
(50) Forconi, M.; Williams, N. H. *Angew. Chem., Int. Ed.* **2002**, *41*, 849−852.
(51) Morio, Y.; Ishikubo, A.; Komiyama, M. *J. Chem. Soc., Chem. Commun.* **1995**, 1793−1794.
(52) Horn, A.; Vencato, I.; Bortluzzi, A. J.; Hoerner, R.; Silva, R. A. N.; Spoganicz, B.; Drago, V.; Terenzi, H.; de Oliveira, M. C. B.; Werner, R.; et al. *Inorg. Chim. Acta* **2005**, *358*, 339−351.
(53) Seo, J. S.; Sung, N.-D.; Hynes, R. C.; Chin, J. *Inorg. Chem.* **1996**, *35*, 7472−7473.
(54) (a) Lanznaster, M.; Neves, A.; Bortoluzi, A. J.; Aires, V. V. E.; Szpoganicz, B.; Terenzi, H.; Severino, P. C.; Fuller, J. M.; Drew, S. C.; Gahan, L. R.; et al. *J. Biol. Inorg. Chem.* **2005**, *10*, 319−332. (b) Peralta, R. A.; Bortoluzzi, A. J.; de Souza, B.; Jovito, R.; Xavier, F. R.; Couto, R. A.; Casellato, A.; Nome, F.; Dick, A.; Gahan, L. R.; et al. *Inorg. Chem.* **2010**, *49*, 11421−11438.
(55) Kanamori, K.; Yamamoto, K.; Okayasu, T.; Matsui, N.; Okamoto, K.; Mori, W. *Bull. Chem. Soc. Jpn.* **1997**, *70*, 3031−3040.
(56) Beurskens, P. T.; Admiraal, G.; Beurskens, G.; Bosman, W. P.; de Gelder, R.; Israel, R.; Smits, J. M. M. *The DIRDIF-99 program system, Technical Reports of the Crystallography Laboratory*; University of Nijmegen: Nijmegen, The Netherlands, 1999.
(57) Sheldrick, G. M. *Acta Crystallogr.* **2008**, *A64*, 121−122.
(58) Frisch, M. J.; Trucks, G. W.; Schlegel, H. B.; Scuseria, G. E.; Robb, M. A.; Cheeseman, J. R.; Scalmani, G.; Barone, V.; Mennucci, B.; Petersson, G. A.; Nakatsuji, H.; Caricato, M.; Li, X.; Hratchian, H. P.; Izmaylov, A. F.; Bloino, J.; Zheng, G.; Sonnenberg, J. L.; Hada, M.; Ehara, M.; Toyota, K.; Fukuda, R.; Hasegawa, J.; Ishida, M.; Nakajima, T.; Honda, Y.; Kitao, O.; Nakai, H.; Vreven, T.; Montgomery, J. A., Jr.; Peralta, J. E.; Ogliaro, F.; Bearpark, M.; Heyd, J. J.; Brothers, E.; Kudin, K. N.; Staroverov, V. N.; Keith, T.; Kobayashi, R.; Normand, J.; Raghavachari, K.; Rendell, A.; Burant, J. C.; Iyengar, S. S.; Tomasi, J.; Cossi, M.; Rega, N.; Millam, N. J.; Klene, M.; Knox, J. E.; Cross, J. B.; Bakken, V.; Adamo, C.; Jaramillo, J.; Gomperts, R.; Stratmann, R. E.; Yazyev, O.; Austin, A. J.; Cammi, R.; Pomelli, C.; Ochterski, J. W.; Martin, R. L.; Morokuma, K.; Zakrzewski, V. G.; Voth, G. A.; Salvador, P.; Dannenberg, J. J.; Dapprich, S.; Daniels, A. D.; Farkas, Ö.; Foresman, J. B.; Ortiz, J. V.; Cioslowski, J.; Fox, D. J. *Gaussian 09*, Revision C.1; Gaussian, Inc.: Wallingford, CT, 2010.
(59) Adamo, C.; Barone, V. *J. Chem. Phys.* **1999**, *110*, 6158−6169.
(60) (a) Dunning, T. H., Jr.; Hay, P. J. *Modern Theoretical Chemistry*; Plenum: New York, 1976; Vol. 3. (b) Hay, P. J.; Wadt, W. R. *J. Chem. Phys.* **1985**, *82*, 270−283. (c) Wadt, W. R.; Hay, P. J. *J. Chem. Phys.* **1985**, *82*, 284−298. (d) Hay, P. J.; Wadt, W. R. *J. Chem. Phys.* **1985**, *82*, 299−310.
(61) (a) Flukiger, P.; Luthi, H. P.; Portmann, S.; Weber, J. *MOLEKEL*; Swiss Center for Scientific Computing: Manno, Switzerland, 2000−2002. (b) Portmann, S.; Luthi, H. P. *Chimia* **2000**, *54*, 766−769.
(62) Kanamori, K. *Coord. Chem. Rev.* **2003**, *237*, 147−161.
(63) Haushalter, R. C.; Wang, Z.; Thompson, M. E.; Zubieta, J. *Inorg. Chim. Acta* **1995**, *232*, 83−89.
(64) Kanamori, K.; Kameda, E.; Kabetani, T.; Suemoto, T.; Okamoto, K.; Kaizaki, S. *Bull. Chem. Soc. Jpn.* **1995**, *68*, 2581−2589.

dx.doi.org/10.1021/ic2024617 | *Inorg. Chem.* 2012, 51, 5026−5036